JSLHR

Research Article

Identifying Predictors of Levator Veli Palatini Muscle Contraction During Speech Using Dynamic Magnetic Resonance Imaging

Eshan Pua Schleif,[a] Catherine M. Pelland,[b] Charles Ellis,[a] Xiangming Fang,[a] Stephen J. Leierer,[a] Bradley P. Sutton,[c] David P. Kuehn,[c] Silvia S. Blemker,[b] and Jamie L. Perry[a]

Purpose: The purpose of this study was to identify predictors of levator veli palatini (LVP) muscle shortening and maximum contraction velocity in adults with normal anatomy.
Method: Twenty-two Caucasian English-speaking adults with normal speech and resonance were recruited. Participants included 11 men and 11 women (M = 22.8 years, SD = 4.1) with normal anatomy. Static magnetic resonance images were obtained using a three-dimensional static imaging protocol. Midsagittal and oblique coronal planes were established for visualization of the velum and LVP muscle at rest. Dynamic magnetic resonance images were obtained in the oblique coronal plane during production of "ansa." Amira 6.0.1 Visualization and Volume Modeling Software and MATLAB were used to analyze images and calculate LVP shortening and maximum contraction velocity.
Results: Significant predictors ($p < .05$) of maximum LVP shortening during velopharyngeal closure included mean extravelar length, LVP origin-to-origin distance, velar thickness, pharyngeal depth, and velopharyngeal ratio. Significant predictors ($p < .05$) of maximum contraction velocity during velopharyngeal closure included mean extravelar length, intravelar length, LVP origin-to-origin distance, and velar thickness.
Conclusions: This study identified six velopharyngeal variables that predict LVP muscle function during real-time speech. These predictors should be considered among children and individuals with repaired cleft palate in future studies.

The levator veli palatini (LVP) muscle is the primary muscle responsible for velar elevation and achieving velopharyngeal (VP) closure, necessary for normal speech production (Perry, 2011a). Magnetic resonance imaging (MRI) has been successfully used to visualize the LVP muscle at rest and during speech production (Mason & Perry, 2017). Studies using MRI have imaged and described the LVP muscle using static VP measures (Mason & Perry, 2017). Comparisons between individuals with cleft palate and those with normal anatomy using static MRI measures suggest significant morphological differences in VP measures during the resting position. These differences include hard palate length (Perry et al., 2018), mean intravelar length (Perry et al., 2018), mean angle of origin (Perry et al., 2018), velar length (Perry et al., 2018; Tian et al., 2010), pharyngeal depth (Perry et al., 2018; Tian et al., 2010), and VP ratio (Satoh et al., 2002; Subtelny, 1957; Tian et al., 2010). It has been shown that alterations to VP anatomical variables can impact LVP muscle activation and closure force (Inouye et al., 2015; Kuehn & Moon, 1998; Moon et al., 2007). However, no one has documented which of these VP variables contribute to LVP function, which may lead to poor VP closure during speech production.

The use of static MRI alone is suboptimal for evaluating VP function because it is acquired at rest or during sustained phonation tasks (Mason & Perry, 2017). The complexity of speech and effect of coarticulation must be considered when evaluating VP function. Therefore, functional assessment of musculature changes should be elicited using real-time speech tasks. MRI with faster image acquisition (dynamic MRI) is needed to capture speech gestures such

[a]East Carolina University, Greenville, NC
[b]University of Virginia, Charlottesville
[c]University of Illinois at Urbana–Champaign
Correspondence to Jamie L. Perry: perryja@ecu.edu

Editor-in-Chief: Bharath Chandrasekaran
Editor: Kate Bunton
Received January 12, 2020
Revision received March 18, 2020
Accepted March 23, 2020
https://doi.org/10.1044/2020_JSLHR-20-00013

Disclosure: *The authors have declared that no competing interests existed at the time of publication.*

as velar elevation, which can occur in less than 100 ms (Kuehn, 1976). Sutton et al. (2009) note that dynamic MRI with image acquisition rate above 10 frames per second is required to capture LVP muscle movement.

To our knowledge, only four studies have reported LVP muscle length during speech production using a dynamic MRI protocol (Ettema et al., 2002; Ha et al., 2007; Pelland et al., 2019; Perry et al., 2014). Only one of these studies reported LVP contraction velocity and examined the effect of four VP variables on LVP contraction: pharyngeal depth, velar length, sagittal angle, and VP port depth (Pelland et al., 2019). Authors concluded that VP port depth was positively correlated with LVP shortening and contraction velocity, and pharyngeal depth was positively correlated with maximum contraction velocity. However, the study by Pelland et al. (2019) was limited by analysis of only six participants and four VP variables. Identifying predictors of LVP function is critical for determining the most favorable VP anatomy required for VP closure (Inouye et al., 2015). Therefore, additional studies are needed to further examine other VP variables that may be predictors of LVP function.

The purpose of this study is to identify predictors of LVP shortening and contraction velocity during speech production by implementing a dynamic MRI and image analysis protocol on a large sample. Information about significant predictors can contribute significantly to surgical considerations, especially for cleft palate repairs. We hypothesize that particular VP variables will have a greater effect on LVP function compared to other VP variables, as shown by simulations using computational modeling (Anderson et al., 2019; Inouye et al., 2015). Specifically, variables such as VP port depth, velar length, and pharyngeal depth are predicted to have a direct and significant effect on LVP contraction during VP closure, while other variables likely play a secondary or assisting role in LVP contraction (Inouye et al., 2015; Pelland et al., 2019; Satoh et al., 2002; Subtelny, 1957). For these reasons, this study includes multiple VP variables related to the velum, LVP muscle, nasopharynx, and hard palate.

Method

Participants

In accordance with the institutional review board at East Carolina University, 22 English-speaking Caucasian adults were recruited to participate in this study. This study only included Caucasian English-speaking adults because evidence suggests race differences in VP function (Perry et al., 2016). Participants included 11 men and 11 women between the ages of 19 and 33 years (M = 22.8, SD = 4.1). Participants were enrolled as part of a larger study that examined sex and race effects on VP variables (Perry et al., 2016). As part of this study, participants were recruited through use of flyers around the community and were monetarily compensated for their participation. All participants indicated no history of craniofacial anomalies, swallowing disorders, sleep apnea, or neurological disorders that may affect measures of structures and their movements. A conversational speech sample lasting approximately 5 min was obtained for all participants. Perceptual rating by a speech-language pathologist with more than 15 years of experience in speech and resonance assessment ensured that all participants presented with oral-to-nasal resonance and articulation skills within normal limits.

MRI

All participants were scanned using a Siemens 3-T Trio MRI scanner and a 12-channel Siemens Trio head coil, while lying in the supine position. An elastic strap attached to the head coil was used to stabilize the head during the scan to limit motion artifact and image blurring. Participants were scanned at rest using three-dimensional (3D) static imaging protocol, consistent with that used in previous MRI investigations of the VP muscles (Perry et al., 2013).

Dynamic images were also acquired according to the imaging protocol described by Perry et al. (2014). A fast gradient echo FLASH (fast low-angle shot) multishot technique was used to obtain dynamic images during speech production. This technique acquired images in the sagittal and oblique coronal planes at 15.8 frames per second (fps) and has been successfully used in dynamic MRI assessments of speech (Perry et al., 2014; Sutton et al., 2010). The sliding window process was utilized to reconstruct the images at a frame rate of 30 fps, also described in previous literature (Perry et al., 2017; Perry et al., 2014). The sliding window reconstruction protocol minimizes repeated temporal information and reduces image blurring that would happen from interpolation (Sutton et al., 2009). Parameters of the MRI protocol are provided in Table 1. During dynamic sequences, participants wore an MR-compatible headset with an attached optical microphone (Dual Channel FOMR-II, Optocacoustics Ltd.). Speech recordings were obtained in real time, consistent with procedures used in previous literature (Bae, Kuehn, Conway, & Sutton, 2011; Perry et al., 2014; Sutton et al., 2010). Participants were instructed to repeat /ɑnsɑ/ 10 times during image acquisition at the pace of one syllable per beat, guided by a metronome playing through the headphones (rate of 120 beats per minute). For MRI methods used in this study, image reconstructions are performed off-line after the MRI data are obtained. Multiple repetitions of the speech sample were obtained to ensure we successfully captured at least one full production. Speech recordings were aligned with dynamic images using an acquisition simulation software provided by the vendor of the MRI scanner. The first production of /ɑnsɑ/ was measured and analyzed to capture the initiation of speech production from resting state.

Speech Task

The speech task /ɑnsɑ/ consists of nasal, nonnasal, and vowel sounds. The vowel–nasal–consonant–vowel (VNCV) speech task allows for analysis of the maximum LVP contraction because the nasal consonant /n/ is produced with the

Table 1. Magnetic resonance imaging (MRI) protocol.

Parameters	Static 3D MRI	Dynamic MRI
Resolution	0.8 mm isotropic	1.875 x 1.875 x 8 mm^3
Field of view	256 × 192 × 153.6 mm^3	240 x 240 x 8 mm^3
Pulse sequence	SPACE: T2 turbo spin echo Variable flip angle	FLASH: gradient echo sequence (GRE) six-shot spiral
Repetition time	2,500 ms	9 ms
Echo time	268 ms Echo train length: 171	Alternating between 1.3 and 1.8 ms
Length of scan	4 min 52 s for 1 static volume	50.5 s for 799 native frame rate images or 1,515 sliding window images at 30 fps

Note. SPACE = sampling perfection with application optimized contrasts using different flip angle evolution; FLASH = fast low-angle shot imaging.

VP port open, followed by /s/, which is a fricative, requiring maximum LVP shortening (Ettema et al., 2002; Pelland et al., 2019). Thus, the /ns/ sequence is beneficial because the dynamic change from nasal consonant to fricative consonant requires rapid LVP movement and contraction. Based on previous research involving velar positioning (Moll, 1962), the following would be expected: highest velar position and greatest VP closure on /s/, lowest velar position and non-VP closure for /n/, and intermediate velar positioning for /a/. The degree of VP closure for /a/ typically depends on the phonetic context with a lower velar position and less VP closure for /a/ in a nasal consonant context and higher velar position and greater VP closure for /a/ in a nonnasal consonant context. This speech task allowed for analysis of LVP shortening and contraction velocity during both VP closure and opening. Visualization of dynamic images enabled investigators to distinguish transitions between fully lowered and fully elevated velar positions. All dynamic images acquired from rest to the end of the first cycle of /ɑnsɑ/ were selected and analyzed.

Image Analyses

All static 3D and dynamic real-time images were imported and measured using a computer software, Amira 6.0.1 Visualization and Volume Modeling Software (Visage Imaging GmbH). Image processing methods for static 3D images were consistent with previously reported methods (Perry, 2011b; Perry & Kuehn, 2007, 2009; Perry et al., 2018, 2014). The midsagittal image plane was established as the image with clear visualization of the midline of the velar body, maximum velar length, posterior nasal spine, and the genu of the corpus collosum (Ettema et al., 2002; Perry et al., 2018). The oblique coronal image was selected as the image slice coursing through the bulk of the velum with clear visualization of the LVP muscle from origin to insertion (Ettema et al., 2002; Perry et al., 2018). VP parameters of interest and methods for obtaining measurements were maintained using prior published studies using MRI data (Bae et al., 2011; Perry, 2011b; Perry et al., 2018; Tian et al., 2010). Description of static VP measures are provided in Table 2 and included commonly reported static VP measures in the midsagittal and oblique coronal plane (Mason & Perry, 2017; Pelland et al., 2019; Perry, 2011b; Perry et al., 2018). Static measures in the oblique coronal plane include average LVP muscle length, mean extravelar length, intravelar length, velar insertion distance, LVP origin-to-origin distance, and mean angle of origin. Static measures in the midsagittal plane include sagittal angle, hard palate length, velar length, velar thickness, pharyngeal depth, retrovelar space, and VP ratio.

Dynamic real-time images were measured on the oblique coronal plane using the method established by Pelland et al. (2019) to quantify LVP muscle contraction during speech production. Reference lines were defined manually using Amira software in high-resolution static images and lower resolution dynamic images. Reference lines marked the lateral edges of the VP port (right lateral line, left lateral line), superior and inferior boundaries of the velum (superior velum line [SVL], inferior velum line [IVL]), LVP origin-to-origin line, and posterior edge of the VP port (posterior pharyngeal wall line; see Figure 1). The coordinates of the reference lines were exported from Amira for each dynamic image with a marked time stamp and then imported into MATLAB (MathWorks, Inc.) for further analysis.

MATLAB was used to assess the LVP length by determining five LVP path vertices: left LVP origin point, right LVP origin point, left velar boundary point (LVBP), right velar boundary point (RVBP), and mid-velum point (MVP). For all subjects, the MVP was determined to be halfway between the SVL and the IVL, leading to the mid-velum factor set at 0.5. The velar boundary point is the intersection of SVL and the right/left lateral line. This method is similar to that used by Pelland et al. (2019). Pelland et al., however, assessed only one side of the LVP muscle and VP port. Given asymmetry in the VP system has been reported among the healthy adult population (Tahmasebifard et al., 2019), our method quantified both sides of the LVP and VP port. The following formulas were used to determine LVP path vertices using the reference lines:

$$\begin{aligned} MVP_x &= (LLL_x + RLL_x)/2 \\ MVP_y &= SVL_y - 0.5 * (SVL_y - IVL_y) \\ LVBP_x &= LLL_x;\ LVBP_y = SVL_y \\ RVBP_x &= RLL_x;\ RVBP_y = SVL_y \end{aligned} \quad (1)$$

Table 2. Description of static magnetic resonance imaging variables.

Velopharyngeal variable	Definition
Midsagittal plane	
Sagittal angle	Angle between vertical line on the anterior border of cervical spine and the oblique line drawn to measure the LVP muscle length
Hard palate length	The distance between the anterior and posterior borders of the hard palate (anterior nasal spine to posterior nasal spine)
Velar length	Curvilinear distance between the posterior nasal spine) and center of the uvula at rest
Velar thickness	Distance from velar knee to velar dimple
Pharyngeal depth	Linear measure created from line drawn from the posterior nasal spine to the posterior pharyngeal wall
Retrovelar space	Linear measure created from line drawn from the velar knee to the posterior pharyngeal wall
Velopharyngeal ratio	(Velar Length) / (Pharyngeal Depth)
Oblique coronal plane	
Average LVP muscle length	Average of right LVP length and left LVP length, where LVP length is the distance from the origin of the muscle at the base of the skull, through the middle of the muscle belly, and to the midline insertion at the velum
Mean extravelar length	Average of right extravelar length and left extravelar length, where extravelar length is the distance from the origin to LVP insertion point into the velum
Intravelar length	Entire length of the LVP muscle that is contained within the body of the velum (right and left segments combined)
Velar insertion distance	Width between where the LVP muscle inserts to the velum
LVP origin-to-origin distance	Width between the two attachments of the levator muscle on both temporal bones
Mean angle of origin	Average of angle created between reference line connecting two origins of the levator muscle and the line drawn to measure the LVP muscle length

Note. LVP = levator veli palatini.

The intravelar segment of the LVP was estimated as the straight-line distance from the LVBP to the MVP to the RVBP. The extravelar segment was estimated as the sum of the straight-line segment from LVBP to the left LVP origin point and the RVBP to the right LVP origin point. The LVP length measurement was the sum of the intra- and extravelar segment lengths, which was calculated for each frame of every dynamic image series.

For each subject, LVP length measurements for the first production of /ɑnsɑ/ were reported across time using percentages based on each subject's LVP resting length to allow for comparisons between participants. Therefore,

Figure 1. Reference lines on static (left) and dynamic (right) image, measured in Amira software. RVBP = right velar boundary point; LVBP = left velar boundary point; MVP = mid-velum point.

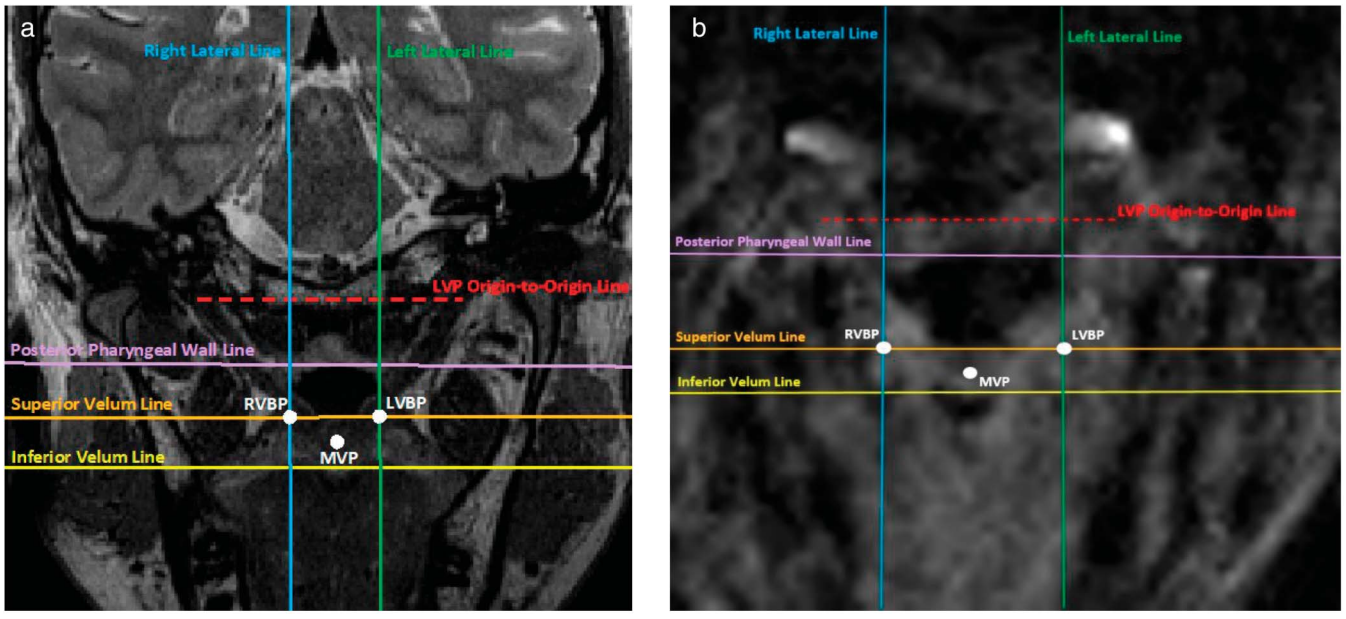

each subject's LVP resting length was 0% LVP shortening. In order to calculate velocity, separate piecewise cubic splines were fit to the LVP length data for the first production of /ɑnsɑ/. Relative LVP muscle velocities were calculated by computing the time derivative of the piecewise function in MATLAB. A positive value for contraction velocity indicated the speed of LVP contraction while a negative value for contraction velocity indicated the speed of LVP relaxation. LVP shortening and maximum contraction velocity was determined by the value with the largest integer for each speech sound (preconsonantal vowel, nasal sound, fricative sound, postconsonantal vowel; see Figure 2). Timestamps from the audio recording and LVP shortening trends were integrated to mark transitions between speech sounds.

Statistical Analysis

All statistical analyses were conducted in IBM SPSS Version 25.0 (IBM Corporation). Multiple linear regression with backward model selection was used to identify VP measures in the static images that were significant predictors of maximum LVP shortening and maximum LVP contraction velocities. Only predictors with p values below .05 were kept in the final model. An analysis of sex and age effects on dependent variables using independent samples t test and Pearson correlations revealed significant associations ($p < .05$). Therefore, sex and age were included in all models to control for age effect and sex differences.

Interrater reliability measures for the dynamic and static measures were obtained using the Pearson product moment correlation ($\alpha = .05$). The primary and secondary raters randomly selected and remeasured data from five randomly selected subjects, for a total comparison of 40 dynamic measures. Interrater reliability for dynamic measures ranged from $r = .901$ to $r = 1.000$. Higher reliability was reported for maximum contraction velocity ($r = .912$) compared to maximum LVP shortening ($r = .901$). Interrater and intrarater reliability for static measures ranged from $r = .85$ to $r = .95$.

Results

Predictors of Maximum LVP Shortening and Contraction Velocity

Results of the multiple linear regression for identification of predictors of LVP shortening in 22 participants are presented in Table 3. Backward model selection (Hocking, 1976) was used to determine the final regression model. Only predictors with p values of less than .05 were kept and included in the final regression model. Significant predictors ($p < .05$) of LVP shortening during speech tasks requiring VP closure (preconsonantal vowel and fricative consonant) include mean extravelar length, LVP origin-to-origin distance, velar thickness, pharyngeal depth, and VP ratio. There were no significant predictors of LVP shortening during speech tasks requiring VP opening (nasal consonant and postconsonantal vowel). Age effect and sex differences were insignificant for all models.

Predictors of LVP contraction velocity found using multiple linear regression in 22 participants are presented in Table 4. Significant predictors ($p < .05$) of LVP contraction velocity during speech tasks requiring VP closure include mean extravelar length, intravelar length, LVP origin-to-

Figure 2. Graphs displaying the results from MATLAB image analysis using measurement coordinates made in Amira. (A) Levator veli palatini (LVP) length measured during /ɑnsɑ/ production. The extravelar and intravelar segment is marked by the 5 points defined using formulas reported. The blue line represents LVP resting (optimal) length, and the red line represents the measured LVP path at maximum LVP shortening. (B) LVP shortening (where 0% shortening indicates LVP at rest) plotted across time (in seconds). The blue line represents the true values, and the black line represents values after separate piecewise cubic splines were fit to the LVP shortening data.

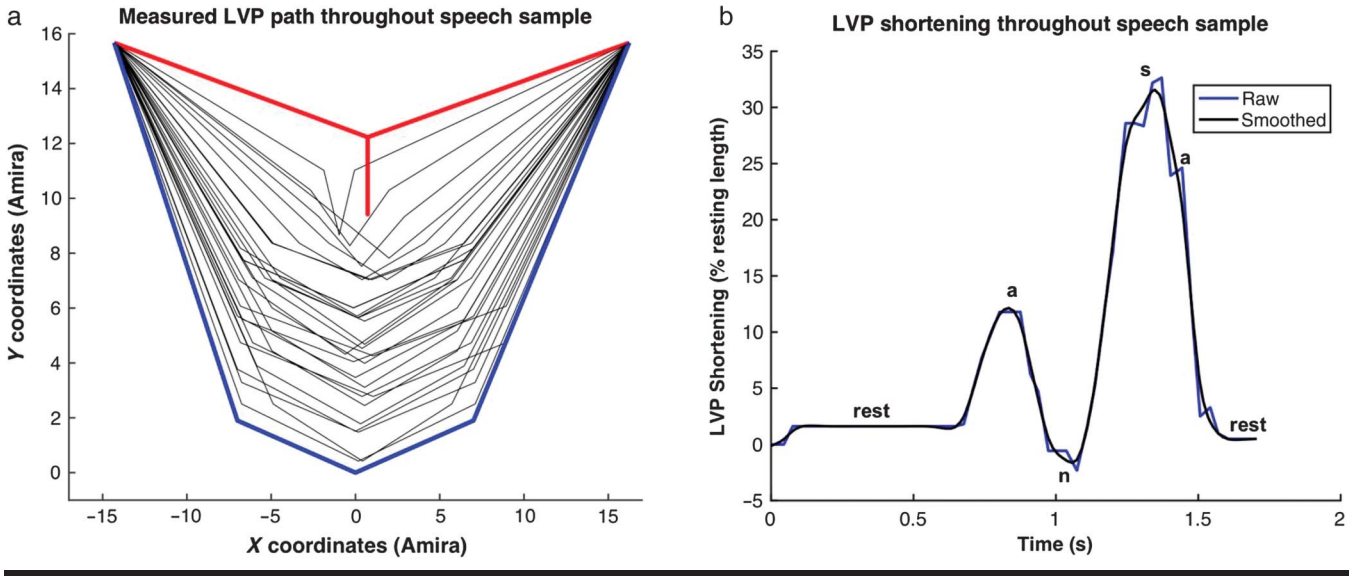

Table 3. Linear regression to determine predictors of levator veli palatini (LVP) muscle shortening.

Speech sound	VP movement	R^2	F(df1, df2)	Coefficients				
				VP static variables (predictors of shortening)	Unstandardized coefficients		t	Sig.
					B	*SE*		
Preconsonantal /a/	VP closing	.485	3.008 (5, 16)	Mean extravelar length	1.685	0.695	2.425	.028*
				LVP origin-to-origin distance	–1.012	0.378	–2.679	.016*
				Velar thickness	–2.048	0.869	–2.358	.031*
/s/	VP closing	.376	2.557 (4, 17)	Pharyngeal depth	1.957	0.640	3.057	.007*
				VP ratio	–46.115	19.914	–2.316	.033*

Note. Reported models are the final models with backward model selection. Only predictors with p values of < .05 were kept in the final model. Age and sex were included in all models to control for age effect and sex differences. Df1 indicates degrees of freedom for model, and df2 is degrees of freedom for the error. VP = velopharyngeal.

*Significant at the .05 level.

origin distance, and velar thickness. Significant predictors of maximum contraction velocity during speech tasks requiring VP opening include hard palate length (p = .026) and velar thickness (p = .043). There were no significant predictors of maximum contraction velocity for production of postconsonantal vowel /a/ and /s/. Age effect was significant only for velocity of preconsonantal /a/. Sex differences were not significant predictors for all models.

Discussion

Five static VP variables were significant for predicting the dynamic variable of LVP shortening during VP closure: mean extravelar length, LVP origin-to-origin distance, velar thickness, pharyngeal depth, and VP ratio (see Table 3). Four static VP variables were significant for predicting the dynamic variable of LVP contraction velocity during VP closure: mean extravelar length, LVP origin-to-origin distance, velar thickness, and intravelar length (see Table 4). Previous literature has shown that increased LVP shortening result in increased LVP activation required and quicker VP fatigue (Inouye et al., 2015). Our results, in conjunction with previous studies, lead to the conclusion that the following changes could result in more favorable LVP function for VP closure: smaller mean extravelar length, larger intravelar length, wider LVP origin-to-origin distance, greater velar thickness, shallower pharyngeal depth, and larger VP ratio.

Our findings indicate that intravelar and extravelar lengths are influential factors of LVP function. As mean extravelar length increases and intravelar length decreases, LVP shortening and velocity increase. This suggests that a decreased extravelar length with an increased intravelar length leads to a more favorable mechanism. Anderson et al. (2019) used computational modeling to also suggest that the intravelar and extravelar portions of the LVP provide different levels of contribution to VP closure. These findings suggest that both intravelar and extravelar lengths are critical in achieving VP closure during speech. These are also areas of interest because reconstruction of the intravelar segment is the surgical site for primary palatoplasty (cleft palate repair). Perry et al. (2013) reported a variability in muscle diameter and circumference in the intravelar

Table 4. Linear regression to determine predictors of maximum levator veli palatini (LVP) contraction velocity.

Speech sound	VP movement	R^2	F(df1, df2)	Coefficients				
				VP static variables (predictors of velocity)	Unstandardized coefficients		t	Sig.
					B	*SE*		
Preconsonantal /a/	VP closing	.715	6.285 (6, 15)	LVP origin-to-origin distance	–0.067	0.030	–2.230	.041*
				Velar thickness	–0.223	0.065	–3.432	.004*
				Mean extravelar length	0.136	0.056	2.414	.029*
				Intravelar length	–0.081	0.028	–2.852	.012*
/n/	VP opening	.367	2.459 (4, 17)	Hard palate length	0.057	0.023	2.442	.026*
				Velar thickness	0.166	0.076	2.187	.043*

Note. Reported models are the final models with backward model selection. Only predictors with p values of < .05 were kept in the final model. Age and sex were included in all models to control for age effect and sex differences. Df1 indicates degrees of freedom for model, and df2 is degrees of freedom for the error. VP = velopharyngeal.

*Significant at the .05 level.

segment in ten healthy adults. In addition, Perry et al. (2014) reported differences in extravelar and intravelar segments between healthy men and women. Further study is needed to determine the effect of these variations on LVP function in the cleft population.

This study found a negative association between LVP origin-to-origin distance and LVP shortening and LVP contraction velocity. We also found that increased velar thickness resulted in decreased LVP shortening and contraction velocity and increased hard palate length resulted in decreased LVP contraction velocity. Previous studies show that greater LVP shortening leads to increased fatigue, as the muscle moves away from its optimal length (Inouye et al., 2015; Pelland et al., 2019). This finding has significant implications indicating that a narrower origin-to-origin distance, thinner velum, and shorter hard palate length lead to a more disadvantageous VP mechanism. This finding is of particular interest for clinical populations such as 22q11.2 deletion syndrome and individuals with repaired cleft palate in which a hallmark feature associated with those who present with hypernasal speech is narrower origin-to-origin distances (Kollara et al., 2019; Ha et al., 2007). In addition, adults with repaired cleft palate demonstrated decreased velar thickness and shorter hard palate length compared to those with normal anatomy (Perry et al., 2018).

Significant predictors of LVP shortening during /s/ production were pharyngeal depth and VP ratio. This study concluded that as pharyngeal depth increases, LVP shortening increases, and as VP ratio increases, LVP shortening decreases. These findings are similar to those reported by Inouye et al. (2015) and Pelland et al. (2019), where a larger VP opening required increased LVP activation and closure force to achieve closure, leading to a more fatigued and less favorable VP mechanism. The predictor variable of VP ratio, calculated as velar length to pharyngeal depth, suggest that pharyngeal depth alone does not always determine LVP function. A longer velar length in the presence of a deep pharynx could decrease the LVP shortening required and decrease the LVP activation and closure force. It should be noted that pharyngeal depth and VP ratio were significant only for predicting LVP shortening during /s/ production, which required greatest LVP shortening and velocity. Perhaps pharyngeal depth and VP ratio measures are variables that differentiate between taxing VP tasks. These findings are consistent with Perry et al. (2018), where adults with healthy anatomy had significantly smaller pharyngeal depth and larger VP ratio when compared to adults with repaired cleft anatomy, even in the absence of abnormal speech characteristics. Further study is needed to examine the difference in LVP shortening and contraction velocity within the cleft population with VP dysfunction.

Comparisons of LVP Shortening and Contraction Velocity With Previous Studies

Similar to Pelland et al. (2019), the four sounds (preconsonantal vowel, nasal sound, fricative sound, postconsonantal vowel) demonstrated varied amounts of LVP shortening and maximum contraction velocities (see Table 5). The greatest LVP shortening was observed during the production of fricative sound /s/, followed by postconsonantal vowel, preconsonantal vowel, and nasal sound. Dynamic LVP results from this study are comparable to LVP shortening values reported in previous literature (see Table 6). Similar to prior studies (Ettema et al., 2002; Pelland et al., 2019), LVP shortening becomes progressively greater from rest, nasal, vowels to fricatives. The greatest LVP shortening was observed during production of voiceless fricative /s/, which has been described as the phoneme requiring high intra-oral air pressure level and strongest LVP activation potentials (Lubker et al., 1970). The maximum LVP shortening for /s/ is comparable to peak velar displacement reported by Karnell et al. (1988), which occurred during oral consonant production followed by velar lowering during vowel production.

Variation within LVP shortening of vowel production could be attributed to differences in speech stimuli due to the influence of phonetic context on velar positioning and coarticulation (Kuehn, 1976). The LVP shortening reported by Pelland et al. (2019) was averaged between low vowels /æ/ and high vowel /i/ and elicited in isolation, while the LVP shortening reported in the current study was low vowel /ɑ/, elicited in preconsonantal and postconsonantal position of VNCV sequence. Ettema et al. (2002) reported that high vowels showed more LVP shortening compared to low vowels. Another possible explanation may be that features of anticipation, assimilation, and coarticulation contributed to the variation in LVP shortening during vowel production, where decreased LVP shortening is observed in vowels preceding a nasal consonant /n/, as observed in the current study and the study of Perry et al. (2014). This is consistent with the velar positioning results of Moll (1962) in which the vowel /a/ preceding /n/ would be in a lower position due to anticipatory coarticulation of /n/ compared to that for the postconsonantal /a/, which would be in a somewhat higher position due to carryover coarticulation from the nonnasal consonant /s/ (see Table 5). Additionally, observations of LVP movement in this study is consistent with the spatial–temporal model by Bell-Berti (1980) where velar position of the same vowel varies based on surrounding consonant

Table 5. Maximum levator veli palatini (LVP) shortening and maximum contraction velocity.

Speech sample	*n*	Maximum LVP shortening (% rest)		Maximum contraction velocity (muscle lengths/s)	
		M	*SD*	*M*	*SD*
Pre_a	22	10.25	6.58	1.10	0.61
n	22	2.37	5.86	–0.73	0.56
s	22	19.95	6.30	1.54	0.71
Post_a	22	15.58	7.55	–1.27	0.77

Note. Pre_a = preconsonantal vowel; Post_a = postconsonantal vowel.

Table 6. Maximum levator veli palatini (LVP) shortening (% rest) in comparison with previous literature examining noncleft adults.

	LVP shortening (% rest)					
	Current study		Pelland et al. (2019)		Perry et al. (2014)	Ettema et al. (2002)
Speech sample	*M*	*SD*	*M*	*SD*	*M*	*M*
Vowels (preconsonantal)	10.2	6.6	14.0	4.2	14.0	13.9
Vowels (postconsonantal)	15.6	7.6	—	—	16.0	—
Nasals	2.4	5.9	10.0	4.2	5.0	1.5
Fricatives	19.9	6.3	18.0	4.8	13.0	19.0
Participants	22 adults (11 men, 11 women)		6 adults (3 men, 3 women)		10 adults (10 men)	10 adults (5 men, 5 women)
Speech stimuli	/ɑnsɑ/		/sʌ/, /fʌ/, /mʌ/, /nʌ/, /æ/, /i/		/ɑnsɑ/	Varying VCV and VCCV sequences

Note. Em dashes indicate data not reported. V = vowel; C = consonant.

sounds. Nevertheless, all values of LVP shortening for vowels fell within 1 *SD* of findings reported in the current study.

A comparison of maximum LVP contraction velocity results from the current study and velocity values reported by Pelland et al. (2019) is presented in Table 7. The trend of fricatives showing the highest contraction velocity, followed by vowels and nasals, is observed in both studies. Differences between velocity values can be attributed to differences in speech tasks elicited. The negative value in velocity observed for the nasal consonant and postconsonantal vowel in the current study indicates decreasing LVP length or LVP muscle relaxation. This study elicited VNCV sequence /ɑnsɑ/ at the rate of 120 syllables per minute. In contrast, Pelland et al. elicited CV sequence /sʌ, fʌ, mʌ, nʌ/ and vowels /æ, i/ at the rate of approximately 60 syllables per minute. While speaking rate does not alter the pattern of velar movement (Karnell et al., 1988), peak velar elevation can be influenced by consonant duration (Bell-Berti, 1980). Observations in this study are consistent with findings by Bell-Berti (1980), as variable consonant production duration by different participants resulted in a range of maximum LVP shortening and contraction velocity measures. The differences in velocities of nasal consonant can also be explained by the difference in producing /nʌ/ from rest and producting /ɑn/. The increased fricative velocity observed in this study is likely attributed to a rapid LVP shortening required for production of /ns/, moving from least LVP shortening to most LVP shortening in a short time.

Table 7. Maximum contraction velocity in comparison with study by Pelland et al. (2019).

Speech sample	Pelland et al. (2019)		Current study	
	M	*SD*	*M*	*SD*
Vowels (pre_a)	0.40	0.15	1.10	0.61
Vowels (post_a)			–1.27	0.77
Nasals	0.39	0.21	–0.73	0.56
Fricatives	0.74	0.35	1.54	0.71

Lastly, this study acquired images at 15.8 fps and used a sliding window method to reconstruct the images to achieve 30 fps while Pelland et al. (2019) captured images at 18.2 fps and did not use image reconstruction. A faster frame rate enabled analysis of muscle lengths changes within a shorter range of time, every 33.33 ms. Velar elevation can occur in less than 100 ms, requiring at least 10 fps to capture LVP movement (Kuehn, 1976; Narayanan et al., 2004; Perry et al., 2014; Sutton et al., 2010). Previous studies utilizing nasoendoscopy reported peak velar elevation occurring 75 ms before the acoustic onset of the vowel (Bell-Berti, 1980) and a mean timing of peak velar displacement achieved between 20 and 27 ms after acoustic onset (Karnell et al., 1988). This study calculated velocity from images obtained every 33.33 ms, which could result in underestimating the true measure of LVP contraction velocity. Further exploration is needed to determine the true velocity of LVP contraction, which will be enabled by further advancements in MRI that have allowed for up to 166 fps, one image every 6.02 ms (Fu et al., 2017).

Study Limitations

This study was limited by a sample size of 22 and examined only the healthy Caucasian adult population. The small sample size may limit the strength of the variables determined as significant predictors. Sex differences were not significant for predicting LVP function. Further examination with a larger sample size for sex comparisons across different ages and races is needed. Individuals with cleft anatomy and normal and abnormal speech should be examined to confirm the relevance of findings in the clinical population. The use of dynamic MRI protocol is currently limited to research settings and not readily available to clinical sites. More development is needed to transfer the use of dynamic MRI into clinical protocols. Further consideration must be given to the variability in an individual's speech production across repetitions, as only the first cycle of /ɑnsɑ/ was analyzed in this study. Furthermore, limitations of this study also include the low-resolution dynamic images and a sliding window frame rate of 30 fps. Advancements in dynamic MRI can achieve up to 166 fps with a

$2.2 \times 2.2 \times 5.0$ mm^3 spatial resolution (Fu et al., 2017). Manual analysis of dynamic imaging is an extremely time-consuming process because it requires measuring hundreds of sequential images. Developments are needed to simplify or automate a reliable image analysis procedure.

Conclusion

This study identified six static VP measures that predict LVP function during VP closure: mean extravelar length, intravelar length, LVP origin-to-origin distance, velar thickness, pharyngeal depth, and VP ratio. Dynamic MRI and a novel method established by Pelland et al. (2019) for assessing LVP function during speech production was successfully implemented on a larger sample. Results from this study provide knowledge about which VP structures influence LVP muscle function and VP closure during real-time speech. Although this protocol is not readily available for clinical MRI scanners, this article supports the benefits of dynamic MRI, which can capture speech production and provide information that static MRI cannot provide.

Acknowledgments

This study was made possible by Grant 1R03DC009676-01A1 from the National Institute on Deafness and Other Communicative Disorders. Its contents are solely the responsibility of the authors and do not necessarily represent the official views of the National Institutes of Health. The first author would also like to acknowledge God as the Giver of life and Jesus Christ the Savior, who has been her help in the writing of this article.

References

Anderson, P., Fels, S., Stavness, I., Pearson, W. G., & Gick, B. (2019). Intravelar and extravelar portions of soft palate muscles in velic constrictions: A three-dimensional modeling study. *Journal of Speech, Language, and Hearing Research, 62*(4), 802–814. https://doi.org/10.1044/2018_JSLHR-S-17-0247

Bae, Y., Kuehn, D. P., Conway, C. A., & Sutton, B. P. (2011). Real-time magnetic resonance imaging of velopharyngeal activities with simultaneous speech recordings. *The Cleft Palate–Craniofacial Journal, 48*(6), 695–707. https://doi.org/10.1597/09-158

Bae, Y., Kuehn, D. P., Sutton, B. P., Conway, C. A., & Perry, J. L. (2011). Three-dimensional magnetic resonance imaging of velopharyngeal structures. *Journal of Speech, Language, and Hearing Research, 54*(6), 1538–1545. https://doi.org/10.1044/1092-4388(2011/10-0021)

Bell-Berti, F. (1980). Velopharyngeal function: A spatial–temporal model. In N. J. Lass (Ed.), *Speech and language* (Vol. 4, pp. 291–316). Elsevier. https://doi.org/10.1016/B978-0-12-608604-1.50012-4

Ettema, S. L., Kuehn, D. P., Perlman, A. L., & Alperin, N. (2002). Magnetic resonance imaging of the levator veli palatini muscle during speech. *The Cleft Palate–Craniofacial Journal, 39*(2), 130–144. https://doi.org/10.1597/1545-1569_2002_039_0130_mriotl_2.0.co_2

Fu, M., Barlaz, M. S., Holtrop, J. L., Perry, J. L., Kuehn, D. P., Shosted, R. K., Liang, Z.-P., & Sutton, B. P. (2017). High-frame-rate full-vocal-tract 3D dynamic speech imaging. *Magnetic Resonance in Medicine, 77*(4), 1619–1629. https://doi.org/10.1002/mrm.26248

Ha, S., Kuehn, D. P., Cohen, M., & Alperin, N. (2007). Magnetic resonance imaging of the levator veli palatini muscle in speakers with repaired cleft palate. *The Cleft Palate–Craniofacial Journal, 44*(5), 494–505. https://doi.org/10.1597/06-220.1

Hocking, R. R. (1976). A Biometrics invited paper. The analysis and selection of variables in linear regression. *Biometrics, 32*(1), 1–49. https://doi.org/10.2307/2529336

Inouye, J. M., Perry, J. L., Lin, K. Y., & Blemker, S. S. (2015). A computational model quantifies the effect of anatomical variability on velopharyngeal function. *Journal of Speech, Language, and Hearing Research, 58*(4), 1119–1133. https://doi.org/10.1044/2015_JSLHR-S-15-0013

Karnell, M. P., Linville, R. N., & Edwards, B. A. (1988). Variations in velar position over time: A nasal videoendoscopic study a nasal videoendoscopic study. *Journal of Speech, Language, and Hearing Research, 31*(3), 417–424. https://doi.org/10.1044/jshr.3103.417

Kollara, L., Baylis, A. L., Kirschner, R. E., Bates, D. G., Smith, M., Fang, X., & Perry, J. L. (2019). Velopharyngeal structural and muscle variations in children with 22q11.2 deletion syndrome: An unsedated MRI study. *The Cleft Palate–Craniofacial Journal, 56*(9), 1139–1148. https://doi.org/10.1177/1055665619851660

Kuehn, D. P. (1976). A cineradiographic investigation of velar movement variables in two normals. *The Cleft Palate Journal, 13*(2), 88–103.

Kuehn, D. P., & Moon, J. B. (1998). Velopharyngeal closure force and levator veli palatini activation levels in varying phonetic contexts. *Journal of Speech, Language, and Hearing Research, 41*(1), 51–62. https://doi.org/10.1044/jslhr.4101.51

Lubker, J. F., Fritzell, B., & Lindqvist-Gauffin, J. (1970). Velopharyngeal function: An electromyographic study. *Speech Transmission Laboratory Quarterly Progress and Status Report, 11*(4), 9–20.

Mason, K., & Perry, J. (2017). The use of magnetic resonance imaging (MRI) for the study of the velopharynx. *SIG 5 Perspectives on Craniofacial and Velopharyngeal Disorders, 2*(5), 35–52. https://doi.org/10.1044/persp2.SIG5.35

Moll, K. L. (1962). Velopharyngeal closure on vowels. *Journal of Speech and Hearing Research, 5*(1), 30–37. https://doi.org/10.1044/jshr.0501.30

Moon, J. B., Kuehn, D. P., Chan, G., & Zhao, L. (2007). Induced velopharyngeal fatigue effects in speakers with repaired palatal clefts. *The Cleft Palate–Craniofacial Journal, 44*(3), 251–260. https://doi.org/10.1597/06-098

Narayanan, S., Nayak, K., Lee, S., Sethy, A., & Byrd, D. (2004). An approach to real-time magnetic resonance imaging for speech production. *The Journal of the Acoustical Society of America, 115*(4), 1771–1776. https://doi.org/10.1121/1.1652588

Pelland, C. M., Feng, X., Borowitz, K. C., Meyer, C. H., & Blemker, S. S. (2019). A dynamic magnetic resonance imaging–based method to examine in vivo levator veli palatini muscle function during speech. *Journal of Speech, Language, and Hearing Research, 62*(8), 2713–2722. https://doi.org/10.1044/2019_JSLHR-S-18-0459

Perry, J. L. (2011a). Anatomy and physiology of the velopharyngeal mechanism. *Seminars in Speech and Language, 32*(2), 83–92. https://doi.org/10.1055/s-0031-1277712

Perry, J. L. (2011b). Variations in velopharyngeal structures between upright and supine positions using upright magnetic resonance imaging. *The Cleft Palate–Craniofacial Journal, 48*(2), 123–133. https://doi.org/10.1597/09-256

Perry, J. L., Kotlarek, K. J., Sutton, B. P., Kuehn, D. P., Jaskolka, M. S., Fang, X., Point, S. W., & Rauccio, F. (2018). Variations in velopharyngeal structure in adults with repaired cleft palate. *The Cleft Palate–Craniofacial Journal, 55*(10), 1409–1418. https://doi.org/10.1177/1055665617752803

Perry, J. L., & Kuehn, D. P. (2007). Three-dimensional computer reconstruction of the levator veli palatini muscle in situ using magnetic resonance imaging. *The Cleft Palate–Craniofacial Journal, 44*(4), 421–423. https://doi.org/10.1597/06-137.1

Perry, J. L., & Kuehn, D. P. (2009). Magnetic resonance imaging and computer reconstruction of the velopharyngeal mechanism. *The Journal of Craniofacial Surgery, 20*(8), 1739–1746. https://doi.org/10.1097/SCS.0b013e3181b5cf46

Perry, J. L., Kuehn, D. P., & Sutton, B. P. (2013). Morphology of the levator veli palatini muscle using magnetic resonance imaging. *The Cleft Palate–Craniofacial Journal, 50*(1), 64–75. https://doi.org/10.1597/11-125

Perry, J. L., Kuehn, D. P., Sutton, B. P., & Fang, X. (2017). Velopharyngeal structural and functional assessment of speech in young children using dynamic magnetic resonance imaging. *The Cleft Palate–Craniofacial Journal, 54*(4), 408–422. https://doi.org/10.1597/15-120

Perry, J. L., Kuehn, D. P., Sutton, B. P., & Gamage, J. K. (2014). Sexual dimorphism of the levator veli palatini muscle: An imaging study. *The Cleft Palate–Craniofacial Journal, 51*(5), 544–552. https://doi.org/10.1597/12-128

Perry, J. L., Kuehn, D. P., Sutton, B. P., Gamage, J. K., & Fang, X. (2016). Anthropometric analysis of the velopharynx and related craniometric dimensions in three adult populations using MRI. *The Cleft Palate–Craniofacial Journal, 53*(1), 1–13. https://doi.org/10.1597/14-015

Satoh, K., Wada, T., Tachimura, T., & Shiba, R. (2002). The effect of growth of nasopharyngeal structures in velopharyngeal closure in patients with repaired cleft palate and controls without clefts: A cephalometric study. *British Journal of Oral and Maxillofacial Surgery, 40*(2), 105–109. https://doi.org/10.1054/bjom.2001.0749

Subtelny, J. D. (1957). A cephalometric study of the growth of the soft palate. *Plastic and Reconstructive Surgery, 19*(1), 49–62. https://doi.org/10.1097/00006534-195701000-00007

Sutton, B. P., Conway, C. A., Bae, Y., Brinegar, C., Liang, Z.-P., & Kuehn, D. P. (2009, September). *Dynamic imaging of speech and swallowing with MRI*. Paper presented at the 31st Annual International Conference of the IEEE Engineering in Medical & Biology Society, Minneapolis, MN, United States. https://doi.org/10.1109/IEMBS.2009.5332869

Sutton, B. P., Conway, C. A., Bae, Y., Seethamraju, R., & Kuehn, D. P. (2010). Faster dynamic imaging of speech with field inhomogeneity correlated spiral fast low angle shot (FLASH) at 3T. *Journal of Magnetic Resonance Imaging, 32*(5), 1228–1237. https://doi.org/10.1002/jmri.22369

Tahmasebifard, N., Ellis, C., Rothermich, K., Fang, X., & Perry, J. L. (2019, November). *Evaluation of the levator veli palatini muscle asymmetry in noncleft population using MRI and correlation to nasopharyngoscopy findings*. Paper presented at the meeting of American Speech-Language-Hearing Association, Orlando, FL.

Tian, W., Li, Y., Yin, H., Zhao, S.-F., Li, S., Wang, Y., & Shi, B. (2010). Magnetic resonance imaging assessment of velopharyngeal motion in Chinese children after primary palatal repair. *The Journal of Craniofacial Surgery, 21*(2), 578–587.